An Improved Method of Pre-Deblurring Digital Images Towards the Pre-Compensation of Refractive Errors

MIGUEL ALONSO JR.[1] and ARMANDO BARRETO[1,2]
[1]Electrical & Computer Engineering Department
[2]Biomedical Engineering Department
Florida International University
Miami, Florida, 33174
USA
malons05@fiu.edu, barretoa@fiu.edu http://dsplab.eng.fiu.edu

Abstract: - Current technology in optics makes it possible to compensate for some common visual limitations (up to second order visual impairments) through spectacles or contact lenses. Current wavefront sensing techniques provide a model of these visual limitations through the Point Spread Function (PSF) of the eye. This model could be used to pre-compensate the images displayed on computer screens to counter the distortion in the user's eye. Furthermore, this correction can be applied to visual limitations for which current optical techniques are inappropriate, such as keratoconus, or other high-order visual limitations. This paper outlines a mechanism for such pre-compensation, and shows results obtained using the PSF of a -6.0D defocus to simulate an eye with severe visual limitations. Additionally, the approach is improved by a novel edge-masked contrast enhancement method to redress the contrast loss introduced by the -6.0D lens.

Key-Words: - Point Spread Function, PSF, Wavefront Aberration, Histogram, Edge Masking

1 Introduction

The sense of sight is a vital component of the mechanisms used by humans to perceive and interact with their environment. Humans have advanced visual capabilities that include high resolution, and the perception of depth and color [1]. Humans rely so heavily on the sense of sight that, when it is impaired by age or disease, it limits a person's ability to perform task that are otherwise thought of as ordinary. In particular, in this age when computers provide our gateway to the information technology infrastructure that supports so many of our daily activities, restrictions to computer access imposed by the user's visual limitations are a significant concern.

On the other hand, the perception of images displayed on a computer screen represents a special context in which the visual abilities of the user are exercised, and, most importantly, offes special opportunities for its improvement. This paper describes a method of pre-compensation of computer images aimed at matching them with the visual capabilities of the user to improve the visual perception process.

The visual perception of an external image, or object, is achieved by the formation of a corresponding image in the retina of the viewer, inside his/her eye [2]. Unfortunately, under certain circumstances the natural visual system of some individuals does not map the image of the objects viewed onto their retinas with complete accuracy. Instead, for every point in the object viewed, light is projected on a finite area of the retina, constituting a blur. When the complete object viewed is considered, the superposition of blurs projected onto the retina causes the perception of an "out-of-focus" image of the object. This deviation of the ideal situation, i.e., in which each point of the object viewed causes the stimulation of a "point" in the retina, therefore rendering a "focused" image of the complete object viewed, can also be modeled in terms of the light wavefront caused by each point in the object. In the ideal case, light would emerge from the pupil, in its way through the eye, in a perfectly spherical pattern that would collapse onto a single point on the retina. In reality, however, the optics of the eye produces wavefronts, which depart from that ideal pattern. The deviations from the ideal spherical wavefront pattern are modeled by the "wavefront aberration function", which characterizes the different types of visual limitations, such as myopia, hyperopia and astigmatism.

In practice, the wavefront aberration function is expressed as a combination of Zernike polynomials, of increasing orders. The Zernike polynomials are two-dimensional functions that form a complete orthogonal basis set defined on the unit disc. They have been used in optical engineering for over 60 years, [6], [7], and [8].

Recently, the Zernike polynomials have

been applied to the characterization of aberrations of the human eye [9], [10], and [11]. Simple wavefront aberration profiles, such as those associated with myopia, hyperopia and astigmatism require only the consideration of Zernike polynomials up to second order. These low-order visual impairments are commonly addressed by interposing optical systems (spectacles, contact lenses) between the object and the viewer, which modify the external images, before they effectively reach the viewer's eye.

There are cases, however, in which the aberration of the eye is much more complex and does not lend itself to modeling by first or second order Zernike polynomials. These types of aberrations require the inclusion of higher order terms (third order or higher) to obtain an accurate model. With the recent advances in wavefront sensing technology, it is now feasible to accurately model the high-order aberrations present in an individual's eye. This is especially important for individuals for whom there is currently no viable vision correction alternative.

In contrast with the optical correction of visual limitations, the approach described here is based on modifying the image at its source, i.e., in applying image processing modifications on the image to be displayed on-screen before it is shown to the user, using the knowledge of his/her wavefront aberration function. The aim of the pre-compensation proposed is to modify the intended display image in a way that is opposite to the effect of the wavefront aberration of the eye. Once this is achieved, the result is displayed to the viewer so that the effect of the wavefront aberration in the viewer's eye will "cancel" the pre-compensation, resulting in the projection of an undistorted version of the intended image on the retina.

2 Wavefront Aberrations and Zernike Model

2.1 Imaging in the Human Eye as a Convolution Process

A recent shift in the interpretation of optics has been in the characterization of optical systems, including the human eye, as linear, shift invariant systems described by their point spread function (PSF) [2]. Therefore, the eye can be characterized by its PSF, T(x, y), and the retinal image, R(x, y), can be found by convolving (denoted by $\otimes$) the input to the system, the image of the object to be seen, I(x, y), with the PSF of the eye:

$$R(x,y) = I(x,y) \otimes T(x,y) \tag{1}$$

When viewing a computer screen, the real world image, I(x, y), is stored as a digital image, DI(x, y), which will be displayed to the user. The retinal image will be formed by convolution of the on-screen image and the PSF of the viewer's eye:

$$R(x,y) = DI(x,y) \otimes T(x,y) \tag{2}$$

In this case, however, the on-screen image to be displayed to the user can be manipulated in advance. If the inverse PSF of the viewer's eye, T^{-1} (x, y), could be defined, then an image, RD(x,y), which is the result of convolving the intended digital image, DI(x, y), with this inverse function could be shown to the viewer:

$$RD(x,y) = DI(x,y) \otimes T^{-1}(x,y) \tag{3}$$

Under these circumstances, substituting the ordinary DI(x,y) with the pre-compensated RD(x,y), in (2):

$$R(x,y) = \{DI(x,y) \otimes T^{-1}(x,y)\} \otimes T(x,y) = DI(x,y) \tag{4}$$

This means that the user would perceive in R(x,y) an undistorted version of the intended digital image, DI(x,y). The image represented by the braces in (4) can also be considered to be the result of deconvolving the PSF, T(x,y), from the intended image, DI(x,y), yielding the pre-compensated image to be displayed to the viewer. In practice, the deconvolution process may be performed more efficiently in the frequency domain, as discussed below. In any case, it is clear that, in order to obtain RD(x, y) the PSF of the eye must be known or estimated.

2.2 Evaluation of the PSF of the Human Eye

The PSF of the human eye can be found indirectly through what is known as the wavefront aberration function, W(x, y). This function represents the deviation of the light wavefront from a purely spherical pattern as it passes the pupil on its way to the retina [3]. In an unaberrated eye, the refracted light is organized in the form of a uniform spherical wavefront, converging to the paraxial focal point on the retina.

It should be noted that, even if the focusing elements of the eye were perfect, i.e., if there were no aberrations present to distort the image, the retinal image would still contain degradation due to

the diffraction of light as it passes through the pupil ("diffraction limited") [2].

Recently developed "Wavefront Analyzers" based on the Hartmann-Shack Principle have made it possible to measure the wavefront aberration function for the human eye.

The wavefront aberration function, W(x,y), is the primary component of the pupil function, P(x,y), which incorporates the complete information about the imaging properties of the optical system [4]. The pupil function is given by the following:

$$P(x,y) = A(x,y)e^{-j\cdot 2\cdot\pi\cdot n\cdot W(x,y)/\lambda} \quad (5)$$

where A(x,y) is the amplitude function describing the relative efficiency of light passing through the pupil (usually given a value of one), n is the index of refraction, and λ is the wavelength of light in a vacuum [3].

According to the Fourier optics relationships in the eye, knowledge of the pupil function can be used to determine the optical transfer function, OTF, which is "one of the most powerful descriptors of imaging performance for an optical system" [3]. The OTF is a complex function whose magnitude is the modulation transfer function (MTF) and whose phase is the phase transfer function (PTF) [3].

The OTF can be found by convolving the pupil function, P(x,y), with its complex conjugate, P*(-x,-y) [2] and [3]:

$$O(fx,fy) = P(x,y) \otimes P^*(-x,-y) \quad (6)$$

which is equivalent of saying that the OTF is the autocorrelation of the pupil function. The PSF and the OTF are a Fourier transform pair [5]:

$$O(fx,fy) = F\{T(x,y)\} \quad (7)$$

As indicated by equations (5), (6), and (7), this characterization of the optics of the eye can be used to determine its PSF and OTF, thus enabling the implementation of the deconvolution concept expressed in equations (3) and (4), as detailed below.

3 Inverse Filtering

Inverse filtering is traditionally used in image processing to restore an image U(x,y) from a degraded image G(x,y), assuming a known degradation function, H(x,y). As stated above, the input and output of any linear system are related through the convolution operator. That is,

$$G(x,y) = U(x,y) \otimes H(x,y) \quad (8)$$

If the Fourier principles of convolution are applied, U(x,y) can be obtained as follows:

$$U(x,y) = F^{-1}\left\{\frac{F\{G(x,y)\}}{F\{H(x,y)\}}\right\} \quad (9)$$

where $F\{\ \}$ and $F^{-1}\{\ \}$ denote the Fourier transform and the inverse Fourier transform, respectively.

In the context of pre-compensation of a digital image to be shown to the viewer, the objective is to deconvolve the PSF of the viewer's eye, T(x, y), from the intended digital image, DI(x, y), in order to derive the pre-compensated display image to show on-screen, RD(x, y). Making the corresponding substitutions in equation (9), the calculation of RD(x, y) is practically accomplished as:

$$RD(x,y) = F^{-1}\left\{\frac{F\{DI(x,y)\}}{F\{T(x,y)\}}\right\} \quad (10)$$

This process is commonly known as inverse filtering in frequency, with its counterpart in space being deconvolution. It should be noted that, according to equation (7), the denominator within the braces of equation (10) is the OTF of the viewer's eye.

However, this implementation of inverse filtering has several limitations, especially for values of the PSF or its frequency counterpart, the OTF, which are close to zero. A common approach to circumvent this problem is the use of Minimum Mean Square Error (Weiner) filtering [12]. In the context of the problem at hand, this approach obtains the pre-compensated image as:

$$RD(fx,fy) = \left[\frac{1}{T(fx,fy)}\frac{|T(fx,fy)|^2}{|T(fx,fy)|^2 + K}\right]DI(fx,fy) \quad (11)$$

where RD(fx,fy), T(fx,fy), and DI(fx,fy) are the Fourier transforms of RD(x,y), T(x,y), and DI(x,y), respectively. In addition to the limitation of values in the pre-compensated image, the approach indicated in equation (11) helps reduce the impact of modeling or measurement noise inherent to the definition of the eye's PSF. The K factor in equation

(11) should be proportional to the magnitude of the estimation noise in the PSF approximation [12].

4 Results

Figure 2 shows the analytical PSF obtained for a -6.0 D lens, scaled and resized. Additionally, this image has been cropped and padded to match the image size (512x512) of a letter "H" from a standard eye test chart, shown in Figure 1. This is necessary due to the fact that both the image and the PSF need to be of the same size in order to implement the minimum mean square error deconvolution described.

Figure 3 represents the degraded image that would be seen viewing Figure 1 through the blur defined by the PSF in Figure 2. Figure 4 shows the result of applying the pre-compensation process to the image in Figure 1. This is the image that compensates for the aberration introduced by the -6.0 D lens PSF. This image was produced using equation (11) with a K value of 0.0005.

It should be noted that since the deconvolution process produces negative numbers, the pre-compensated image must be shifted up and rescaled to a range [0, 1]. Figure 5 shows the result of viewing the pre-compensated image (Figure 4) through the same blur.

Figure 1-Digital Image of Sloan Letter H (512x512)

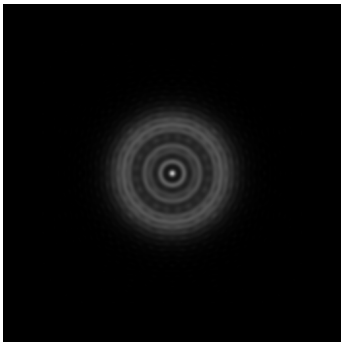

Figure 2-PSF of a -6.0 Diopter Lens

Figure 3-Simulated Blur of Figure 1 using the PSF of Figure 2

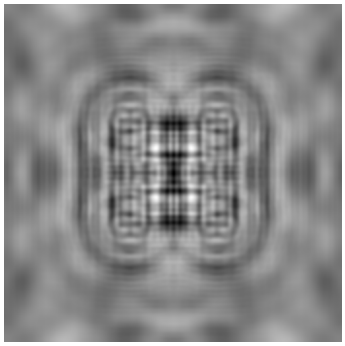

Figure 4-Pre-deblurred Image for the -6.0D PSF, shifted and scaled for display

Figure 5-Simulation of Viewing Figure 4 through the -6.0D lens

5 Edge-mask Contrast Enhancement

It is evident from Figure 5 that, while the pre-compensation process coupled with the shift and scaling operation brings the image of the letter "H" back into focus (compare with Fig. 3), it also introduces a very high loss of contrast. This is apparent from the histograms of the images used (Fig. 10). In general, a low contrast image will have a distribution that is narrow and centered towards the middle of the gray scale [12]. Figure 10-a shows the histogram of Figure 4, the pre-compensated

image. Figure 10-b shows the histogram of Figure 5, the simulation of viewing Figure 4 through the lens. The noticeable deterioration of the contrast in the image reduces its legibility.

While the pre-compensation of areas of the image near the edges is necessary to bring the image back into focus, flat areas of the image have been artificially shifted to a different gray level. To mediate between these opposing requirements, the creation of a mask around the edges is proposed. The final result will be a superposition of areas processed by pre-compensation, near the edges (MASK ON), and areas in the "flat" sections of the image (MASK OFF), where the original image will be replicated.

Construction of the mask is as follows: The edges of the original image are detected, and for each point of the edge, a positive valued, two-dimensional kernel is "stamped" over each point, with the center of the kernel matching the desired point.

The Laplacian of the Gaussian, equation (12), can be used to detect the edges of an image [12].

$$\nabla^2 h(r) = -\left[\frac{r^2 - \sigma^2}{\sigma^4}\right] e^{-\frac{r^2}{2\sigma^2}} \qquad (12)$$

where $r^2 = x^2 + y^2$. Figure 6 shows the result of convolving the image shown in Figure 1 with equation 12.

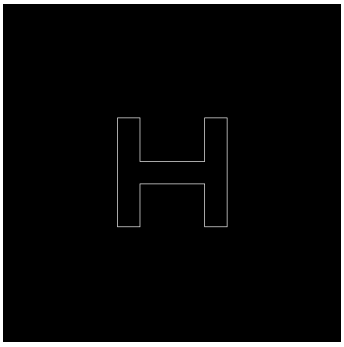

Figure 6-Edges of Figure 1

To obtain the mask, the edge-detected image is convolved with a disk kernel, of specified radius r, given by equation (13).

$$disk(x, y, r) = \begin{cases} 1 & \text{if } x^2 + y^2 \le r^2 \\ 0 & \text{otherwise} \end{cases} \qquad (13)$$

Finally, the edge-mask image is obtained by thresholding the previous result, assigning a value of 1 to all non-zero values. This mask is then used, in conjunction with the original and pre-compensated images, in equation 14 to produce an edge-masked version of Figure 4.

$$RD_{new}(x, y) = DI(x, y) \cdot (1 - MSK(x, y)) + RD(x, y) \cdot (MSK(x, y) \qquad (14)$$

where $RD_{new}(x, y)$ is the edge-masked pre-deblurred image, and $MSK(x, y)$ is the mask shown in Figure 7. The resulting RD_{new} is shown in Figure 8.

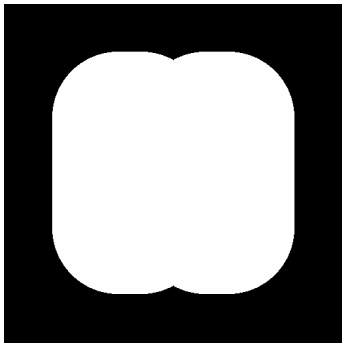

Figure 7- MSK(x,y), Edge mask used to generate Figure 8

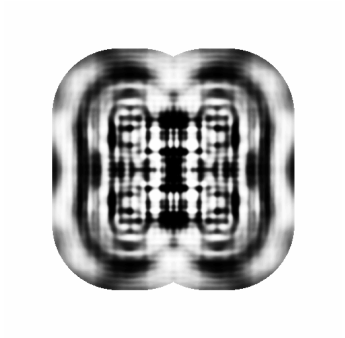

Figure 8-Edge-masked Pre-deblurred Image

Figure 9-Simulation of Viewing Figure 8 through the lens

Figure 8 is the new pre-compensated image, to be displayed on-screen. Figure 9 shows the simulation of viewing Figure 8 through the lens. The improvement in contrast is substantial, as can be seen in Figures 10-c and 10-d, showing the histograms of Figure 8 and Figure 9, respectively.

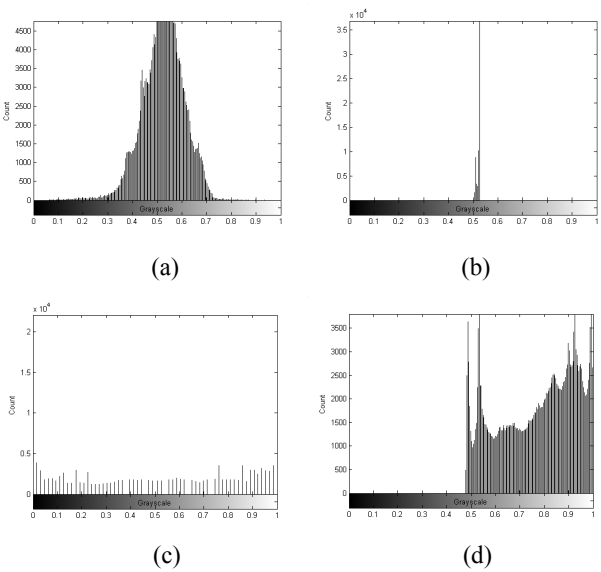

Figure 10-Histograms of (a) Figure 4; (b) Figure 5; (c) Figure 8; and (d) Figure 9

6 Conclusion

This paper has proposed a framework for pre-compensating images before they are displayed to low-vision users on a computer screen in order to address their visual limitations. The results shown in Figure 5, for an example in which a visually limited eye with a strong refractive error was simulated by the PSF corresponding to a –6D lens, underline the potential of the proposed approach. A method of additional processing to increase the final contrast of the images achieved significant improvement in the distribution of grayscale values, as evidenced by Figures 9 and 10. It should be noted that the principle used for these demonstrations can also be applied to higher-order optical aberrations that are not addressed by current visual correction methods.

7 Acknowledgments

This work was sponsored by NSF grants IIS-0308155 and HRD-0317692. Mr. Miguel Alonso Jr. is the recipient of a Graduate Research Fellowship from the National Science Foundation.

References:

[1] X1. Author, Title of the Paper, *International Journal of Science and Technology*, Vol.X, No.X, 19XX, pp. XX-XX.

[2] X2. Author, *Title of the Book*, Publishing House, 19XX

[1] Perry, S.W., H.S. Wong, and L. Guang, *Adaptive Image Processing: A Computational Intelligence Perspective*, CRC Press, New York, 2002.

[2] Thibos, L.N., Formation and Sampling of the Retinal Image, *Chapter 1 in Seeing, A volume in the Handbook of Perception and Cognition Series*, Karen K. De Valois, ed. Academic Press, California, 2000.

[3] Salmon, T.O., Corneal Contribution to the Wavefront Aberration of the Eye, *Doctoral Dissertation, School of Optometry*, Indiana University, 1999.

[4] Williams, C.S., O.A Becklund, *Introduction to the Optical Transfer Function*, John Wiley and Sons, Inc, New York, 1989.

[5] Bracewell, R.N, *Two-Dimensional Imaging*, Prentice-Hall Signal Processing, New Jersey, 1995.

[6] Born, M., and E. Wolf, *Principles of Optics*, 6th Edition, Pergamon Press, Oxford.

[7] Malacara, D., *Optical Shop Testing*, Jon Wiley and Sons, Inc, New York.

[8] Manhan, V., Zernike Circle Polynomials and Optical Aberrations of Systems with Circular Pupils, *Engineering & Laboratory Notes in Optics and Photonics News*, 1994.

[9] Webb, R., Zernike Polynomial description of ophthalmic surfaces, *OSA Technical Digest Series, Ophthalmic and Visual Optics*, 1992.

[10] Liang, J., Grimm, B., Goelz, S. & Bille, J. F., Objective measurement of wave aberrations of the human eye with the use of a Hartmann-Shack wave-front sensor, *J Opt Soc Am A*, 1994.

[11] Liang, J. & Williams, D. R., Effect of higher order aberrations on image quality in the human eye, *OSA Technical Digest Series (Vision Science and Its Applications)*, 1995.

[12] Gonzales, R.C., and R.E. Wood, *Digital Image Processing*, Second Edition, Prentice Hall, New Jersey, 2002.

[13] Sonksen, P. M., and A. J. Macrae, Vision for coloured pictures at different acuities: the Sonksen Picture Guide to Visual Function, *Developmental Medicine Child Neurology*, 29: pp. 337-347, 1987.